


Multiple Solutions When Fitting Excess Gibbs Energy Models and Implications for Process Simulation

Dan Vasiliu^{1,*}, Quirin Göttl^{2,*}, Sönke Bröcker¹, and Jakob Burger²

DOI: 10.1002/cite.202000162

 This is an open access article under the terms of the Creative Commons Attribution License, which permits use, distribution and reproduction in any medium, provided the original work is properly cited.

Excess Gibbs energy models are often fitted to binary experimental data of phase equilibria. Even in the case of two binary parameters fitted to two binary infinite-dilution activity coefficients, multiple solutions for the parameters may occur. The present work shows that this is also true, if more data – like vapor-liquid equilibrium data sets – is used. Chemical systems and conditions are identified that lead to multiple solutions. It is shown that the multiple solutions may lead to significantly different results when the models are used in simulation of separation processes.

Keywords: Excess Gibbs energy models, Multiple solutions, Parameter regression, Process simulation

Received: July 24, 2020; *revised:* September 16, 2020; *accepted:* December 02, 2020

1 Introduction

Models of the excess Gibbs energy (g^E models) are an important class of thermodynamic models for liquid phases and they are intensely used in process simulation of fluid separation processes in the chemical industry. Although old (the versions that are most frequently used today date back to 1960s and 1970s), g^E models are still quite popular. They are a convenient approach to model liquid phase non-ideality by fitting adjustable parameters to different types of experimental data of phase equilibria and excess quantities. From a mathematical standpoint, g^E models – when expressed in intensive variables – are giving the molar excess Gibbs energy g^E as a function of the mole fractions \mathbf{x} and up to two other intensive state variables (typically only the temperature T) and some adjustable parameters τ .

$$g^E = g^E(\mathbf{x}, T, \tau) \quad (1)$$

In systems with more than two components, g^E is typically modeled for all binary subsystems individually, followed by the calculation of g^E for the whole system through empirical interpolation formulas. In all commonly used g^E models, there are only adjustable parameters in the g^E models of the binary subsystems. There are typically no additional adjustable ternary or higher parameters. Thus, fitting binary parameters is the single-most important step when modeling liquid mixtures with g^E models.

The most common case is fitting the two binary parameters, let us say τ_{ij} and τ_{ji} , of a binary g^E model directly to experimental data of the respective binary system ($i + j$). (Note that the binary parameters are not necessarily to be fitted to binary data only. If ternary and higher data is present, it could be considered in the fit of the binary param-

eters by simultaneously considering the interpolation functions.) In this case, Eq. (1) turns into

$$g^E = g^E(x_i, x_j, T, \tau_{ij}, \tau_{ji}) \quad (2)$$

which comes in many different flavors depending on the g^E model in use, e.g., NRTL [1], UNIQUAC [2], Wilson [3], Margules and van Laar [4]. In all cases, g^E is translated via thermodynamic relations, e.g.,

$$RT \ln \gamma_i = \left(\frac{\partial G^E}{\partial n_i} \right)_{n_j, T, p} \quad (3)$$

or

$$\frac{h^E}{RT^2} = - \left(\frac{\partial (g^E/RT)}{\partial T} \right)_{\mathbf{x}, p} \quad (4)$$

to experimentally accessible quantities such as activity coefficients γ_i or excess enthalpies h^E .

Which experimental data to use in the fitting of τ_{ij} and τ_{ji} depends of course firstly on the availability. If available, however, the literature often suggests using the two activity coefficients at infinite dilution γ_i^∞ and γ_j^∞ to determine τ_{ij}

¹Dan Vasiliu, Dr. Sönke Bröcker
dan.vasiliu@evonik.com

Evonik Operations GmbH, Rodenbacher Chaussee 4, 63457 Hanau-Wolfgang, Germany.

²Quirin Göttl, Prof. Jakob Burger
quirin.goettl@tum.de

Technical University of Munich, Campus Straubing for Biotechnology and Sustainability, Laboratory of Chemical Process Engineering, Schulgasse 16, 94315 Straubing, Germany.

and τ_{ji} [5–8]. In this case, one does not have to solve the typical minimization problem of parameter regression. At known experimental temperature, one arrives at two equations

$$\ln\gamma_i^\infty = F_i(\tau_{ij}, \tau_{ji}) \quad (5)$$

$$\ln\gamma_j^\infty = F_j(\tau_{ij}, \tau_{ji}) \quad (6)$$

for the two unknowns τ_{ij} and τ_{ji} . The form of the functions F_i and F_j depends of course on the g^E model that is used. One can solve the system of the two equations – in doubt numerically – and obtain a model that gives exactly the experimental values for γ_i^∞ and γ_j^∞ .

At this point, an important observation is made: most of the commonly used g^E models including NRTL, UNIQUAC and Wilson, lead to highly nonlinear functions F_i and F_j that may lead to multiple solutions for τ_{ij} and τ_{ji} when solving the Eqs. (5) and (6). Initially, Renon and Prausnitz, who came up with NRTL, have (wrongly) denied such multiple solutions, cf. [8]: “At a given temperature T [...] values of $\gamma_1^\infty(T)$ and $\gamma_2^\infty(T)$ uniquely determine values of parameters τ_{12} and τ_{21} .” Later, several authors have studied the equations of specific g^E models in detail and have proven Renon and Prausnitz wrong. Tassios [9] has shown that multiple solutions only occur if both γ_i^∞ and γ_j^∞ are smaller than 1. The existence of multiple solutions was shown for UNIQUAC and Wilson as well [4, 10, 11].

Today, the existence of the multiple solutions is a proved, albeit rather unknown fact in the scientific literature and textbooks. Only very few reference books, e.g., [4, 12–14], mention the occurrence of the multiple solutions. Almost nothing has been reported about the practical implication of these multiple solutions. It is the goal of the present paper to study when exactly multiple solutions occur when fitting parameters of g^E models to binary mixture data and how to possibly avoid them by fitting to diverse data. Furthermore, it is studied how thermodynamic models and process models propagate the deviations between the multiple solutions into the predictions of property data, and ultimately into results of process simulations. It is explored whether the multiple solutions may even lead to significantly different process designs.

2 Occurrence and Avoidance of Multiple Solutions when Fitting Binary Data

In the following, we will focus on one of the most common g^E models: the NRTL model as presented by Renon and Prausnitz [1]. Similar results for other common models like the UNIQUAC or the Wilson model could be obtained following our scheme. The NRTL model for binary systems is given by

$$\frac{g^E}{RT} = x_i x_j \left[\frac{\tau_{ji} G_{ji}}{x_i + x_j G_{ji}} + \frac{\tau_{ij} G_{ij}}{x_j + x_i G_{ij}} \right] \quad (7)$$

where

$$G_{ij} = \exp(-\alpha\tau_{ij}) \quad (8)$$

$$G_{ji} = \exp(-\alpha\tau_{ji}) \quad (9)$$

$$\tau_{ij} = \Delta g_{ij}/(RT) \quad (10)$$

$$\tau_{ji} = \Delta g_{ji}/(RT) \quad (11)$$

Therein, x_i and x_j are the mole fractions of the compounds i and j . The parameter α is often assigned a preset temperature-independent value. We will present our results for several preset values of α . There might arise the question whether the τ or the Δg are the fitting parameters. As a rule, in case of isothermal data one could use the τ and ignore the last two equations, otherwise one would have to stick to the Δg .

For a start, let us look at the problem of determining the binary interaction parameters τ_{ij} and τ_{ji} from the activity coefficients at infinite dilution γ_i^∞ and γ_j^∞ at constant temperature. By using Eq. (3) and considering the limits at infinite dilution, one obtains for NRTL:

$$\ln\gamma_i^\infty = \tau_{ji} + \tau_{ij} \exp(-\alpha\tau_{ij}) \quad (12)$$

$$\ln\gamma_j^\infty = \tau_{ij} + \tau_{ji} \exp(-\alpha\tau_{ji}) \quad (13)$$

To grasp when the system of Eqs. (12) and (13) has multiple solutions, Eq. (12) is solved for τ_{ji} and the result is inserted into Eq. (13). The following equation is obtained.

$$0 = f(\tau_{ij}) = \tau_{ij} - \ln\gamma_j^\infty + (\ln\gamma_i^\infty - \tau_{ij} \exp(-\alpha\tau_{ij})) \times (\exp(-\alpha \ln\gamma_i^\infty) \exp(\alpha\tau_{ij} \exp(-\alpha\tau_{ij}))) \quad (14)$$

Finding solutions for the system (12)–(13) is equivalent to searching roots of the right-hand side of Eq. (14), which is here shortly referred to as the function $f(\tau_{ij})$. Fig. 1 shows a plot of the function $f(\tau_{ij})$ for two combinations of γ_i^∞ and γ_j^∞ , both at $\alpha = 0.3$. The solid curve has three roots, the dashed curve only one. Consequently, the system of

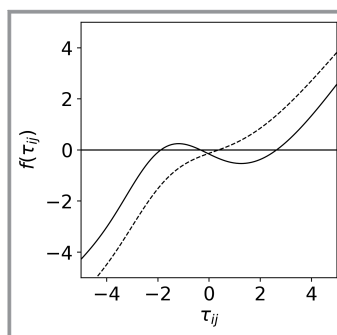


Figure 1. Graph of the right-hand side of Eq. (14) for $\gamma_i^\infty = \gamma_j^\infty = 0.5$; $\alpha = 0.3$ (solid curve) and $\gamma_i^\infty = \gamma_j^\infty = 2$; $\alpha = 0.3$ (dashed curve).

Eqs. (12) and (13) has also three solutions or only one solution, respectively.

A function analysis shows that if at least one of γ_i^∞ or γ_j^∞ is greater than 1, the graph of $f(\tau_{ij})$ is monotonically increasing and the system of Eqs. (12) and (13) has only one unique solution. Every choice of $(\gamma_i^\infty, \gamma_j^\infty) \in (0, 1) \times (0, 1)$ leads to a graph with one maximum and one minimum. To which extent this also leads to three roots of $f(\tau_{ij})$ depends on the value of α . Fig. 2 visualizes the combination of $\gamma_i^\infty, \gamma_j^\infty$ and α , that leads to three solutions. Generally, it holds that the larger the value of α , the larger is the area in the $\gamma_i^\infty, \gamma_j^\infty$ space that leads to three solutions.

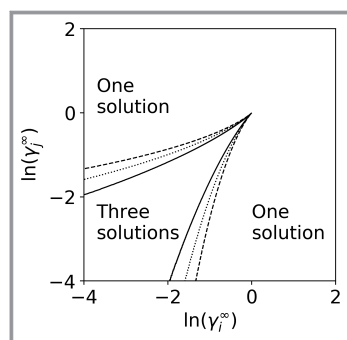


Figure 2. Number of solutions to the problem of fitting the parameters of NRTL to infinite dilution activity coefficients. The boundaries between one and three solutions depend on the value of α : solid ($\alpha = 0.2$), dotted ($\alpha = 0.3$), dashed ($\alpha = 0.47$).

As an example, we have selected the ternary system (acetone, benzene, chloroform), which has an interesting topology in the vapor-liquid equilibrium (VLE) and has, therefore, served as an academic example in many studies in process design and simulation, e.g., [15–17]. The compounds can be conveniently abbreviated by A, B, and C. Tab. 1 shows the binary activity coefficients at infinite dilution in the system at 65 °C, which were calculated using a model from the literature [16]. The values of α were adopted from the same source. Solving the system of Eqs. (12) and (13) leads to one solution in binary AB, and three solutions in BC and AC, cf. Tab. 1. This is in full agreement with the findings presented in Fig. 2. In the system AB, both activity coefficients are greater than 1. In the systems BC and AC, they are both smaller than one and in the region where three solutions are expected. Interestingly,

the three solutions are not necessarily close to each other in the parameter space. Even the signs of the parameter values change from solution to solution for some parameters. Note that Tab. 1 does give the Δg (obtained simply by Eqs. (10) and (11)) and not the τ . In this point, this makes no difference. Later, when the temperature is considered no longer to be constant, it is essential to use the Δg .

Fig. 3 shows the profiles of the activity coefficients for all three solutions in the binary systems AC and BC (system AB is omitted because it has no multiple solutions). Both graphs show the profiles of the two binary activity coefficients. For each activity coefficient there are three curves, one for each solution from Tab. 1. In the system AC (Fig. 3 a), two solutions are very similar, one solution is clearly different from the others. In the system BC (Fig. 3b), all three solutions are quite similar and hard to discern. This indicates that it is quite hard to discriminate the different

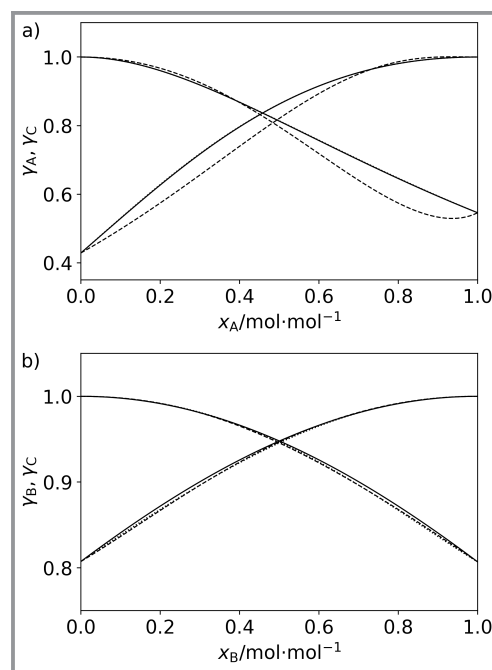


Figure 3. Activity coefficient profiles of two binary subsystems of acetone (A), benzene (B), chloroform (C) at 65 °C; a) system AC, b) system BC. In each subsystems the three model versions from Tab. 1 are shown. The solid, dotted, dashed lines are solutions 1, 2, 3, respectively.

Table 1. Binary activity coefficients at infinite dilutions at 65 °C [16] and NRTL parameters in the system acetone (A), benzene (B), chloroform (C). Solutions in italics are close to the ones reported in [16].

	γ_{ij}^∞	γ_{ji}^∞	α	Solution 1		Solution 2		Solution 3	
				Δg_{ij} [J mol ⁻¹]	Δg_{ji} [J mol ⁻¹]	Δg_{ij} [J mol ⁻¹]	Δg_{ji} [J mol ⁻¹]	Δg_{ij} [J mol ⁻¹]	Δg_{ji} [J mol ⁻¹]
AB	1.63	1.34	0.30	-1252.19	2807.44	-	-	-	-
BC	0.81	0.81	0.30	-283.39	-309.25	3708.77	-3098.14	-3107.70	3728.17
AC	0.43	0.55	0.16	-4221.85	2987.65	-5952.25	5971.37	11916.03	-8428.80

solutions even if more data of the binary activity coefficients at 65 °C would be available. To quantify the extent of the relative differences between the three solutions we used the relative deviation from the mid-range value (RDM), i.e., for a set $X = \{X_i\}_{i < N}$, $RDM(X_i) = (X_i - MRV(X))/MRV(X)$. The mid-range value (MRV) was used as an unbiased reference. MRV is a common statistical estimator of the mean defined as the middle point between the maximum and minimum values of a population, i.e., for a set X , $MRV(X) = 0.5(\text{MIN}(X) + \text{MAX}(X))$. For the system BC, the maximum RDM of the activity coefficients obtained for the three solutions is only $\pm 0.3\%$. The maximum was taken over the entire concentration profiles of both involved activity coefficients.

In the following, it is explored for the system BC which property data would be sufficient to discriminate the three parameter sets. One could for example additionally account for data of the VLE given in T,x,y form at constant pressure. Fig. 4a shows predictions using the three parameters sets from Tab. 1. The VLE is calculated using extended Raoult's law and an ideal vapor phase. The vapor pressure correlations are adopted from [16]. The differences between the three solutions are hardly discernible. Fig. 4b shows the averaged deviation from $K = 14$ experimental data points [18] defined as

$$S_1 = \frac{1}{2K} \sum_{i=1}^K \left[\left| \frac{T^{\text{calc}} - T^{\text{exp}}}{T^{\text{exp}}} \right| + \left| \frac{y_i^{\text{calc}} - y_i^{\text{exp}}}{y_i^{\text{exp}}} \right| \right] \quad (15)$$

plotted as a heat map in the parameter space of the Δg . (In the calculations, pressure and liquid phase composition were specified to the experimental values.) There are three local minima (not marked), which are located very closely to the solutions of Tab. 1 (marked by crosses). Thus, also when T,x,y data are used in the fit, the problem of multiple solution remains for this example. This is not surprising, since there is generally a strong correlation between deviations in activity coefficients and deviations in the T,x,y data.

If the parameter sets from Tab. 1 are used to calculate g^E over the composition at 65 °C, there are no larger differences to observe. However, if other temperatures are used, the three solutions yield different values for g^E . In Fig. 5a, this effect is shown for 120 °C. Thus, different parameter sets that lead to the same activity coefficients at one temperature, can still lead to different temperature dependencies of g^E . This suggests that one has to fit to data sets of different temperatures to discriminate the parameters. Alternatively, one can also consider h^E data (even at constant temperature) to discriminate the multiple solutions. This is shown in Fig. 5b and works, because h^E is correlated with the temperature dependency of g^E . To show how the integrative consideration of h^E eliminates the multiple solutions, another heat map in the Δg space is shown in Fig. 5c. It shows the deviation in the fit according to function S_2 , which equally weighs the deviations from experimental activity coefficients at infinite

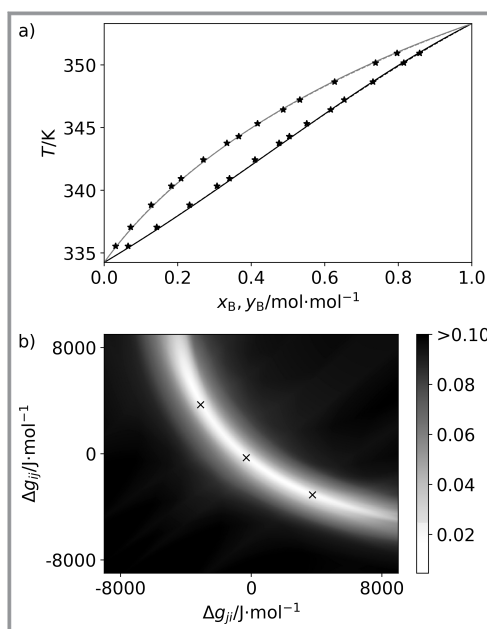


Figure 4. a) Boiling diagram at 101.3 kPa in the system benzene (B) + chloroform (C). Lines are predictions using the three models from Tab. 1. The solid, dotted, dashed lines are solutions 1, 2, 3, respectively. Symbols are experimental data [18]. b) Deviations from experimental data according to Eq. (15) for varying combinations of Δg_{ij} in a heat map. Crosses indicate the solutions from Tab. 1.

dilution at 65 °C and deviations from experimental excess enthalpy data at 25 °C:

$$S_2 = \frac{1}{2K} \sum_{i=1}^K \left| \frac{h^{E,\text{calc}} - h^{E,\text{exp}}}{h^{E,\text{exp}}} \right| + \frac{1}{4} \left[\left| \frac{\gamma_B^{\infty,\text{calc}} - \gamma_B^{\infty,\text{exp}}}{\gamma_B^{\infty,\text{exp}}} \right| + \left| \frac{\gamma_C^{\infty,\text{calc}} - \gamma_C^{\infty,\text{exp}}}{\gamma_C^{\infty,\text{exp}}} \right| \right] \quad (16)$$

There is one single minimum (unmarked). The discussion along Fig. 5 shows that using temperature-dependent VLE data or h^E data in the fit removes the multiple solutions for the temperature-independent parameter set. Independent of this finding, we want to stress that even if there is only one solution in the fit, the fit is not very likely to describe several data well at the same time. Insights about the trade-offs between the description qualities of the different data sets can be obtained by considering the fitting problem as multi-objective problem [19,20]. And of course, one would introduce temperature-dependent parameters in many cases to improve the simultaneous description of multiple data sets. Both is, however, out of the scope of the present work.

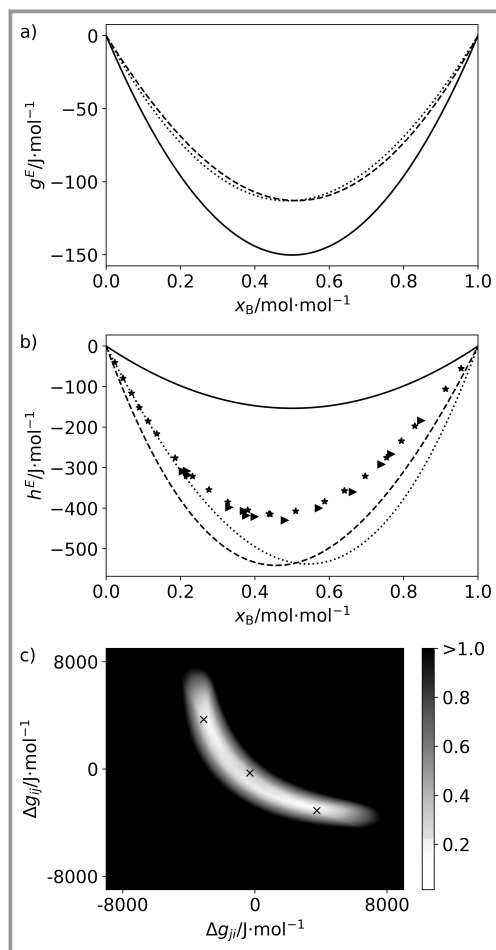


Figure 5. Quantities in the binary system benzene(B) + chloroform (C). a) Molar excess Gibbs energy g^E at 120 °C. b) Molar excess enthalpy h^E at 25 °C. Lines are predictions using the three models from Tab. 1. The solid, dotted, dashed lines are solutions 1, 2, 3, respectively. Symbols are experimental data: ★ [21] and ▲ [22]. c) Deviations from experimental data according to Eq. (16) for varying combinations of Δg_{ij} in a heat map. Crosses indicate the solutions from Tab. 1.

3 Propagation and Amplification of Deviations

If it is not possible to discriminate the multiple solutions described above (e.g., due to missing experimental data), it is interesting to know how the deviations between the multiple solutions propagate when the models are used in simulations of multi-component mixtures. Still – for the sake of brevity – we focus our studies on the multiple solutions in the binary system BC. For the system AC, which also has multiple solutions, we chose the second solution from Tab. 1 and stick with it for now. Fig. 6 shows plots of the activity coefficients of A, B and C at infinite dilution in solutions of the respective other two components. Although the activity coefficients in the binary systems (cf. Fig. 3) are hardly discernible for the three solutions, it is striking that the maximum RDM of the activity coefficients obtained for

the three considered solutions in the ternary system ABC lies between $\pm 18\%$ and $\pm 30\%$, depending on the regarded species. On the one hand, this gives another chance for discrimination of the solutions, e.g., by considering ternary VLE data in the fit. Alternatively, one could argue for and against certain solutions using a molecular point of view, e.g., by assuming that the molecules' association sites behave different in pure and mixed solvents. On the other hand, it shows that the deviations of the different solutions are significantly amplified.

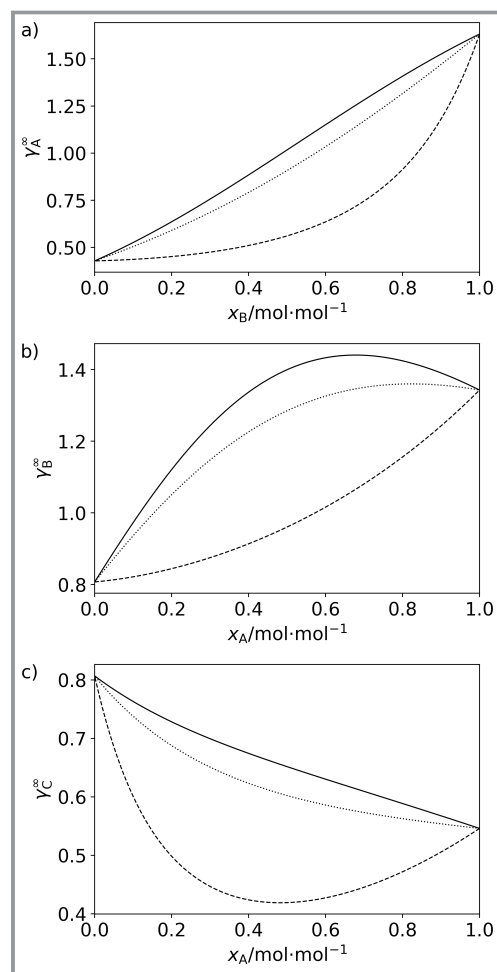


Figure 6. Activity coefficients at infinite dilution γ_i^∞ in the ternary system acetone (A), benzene (B), chloroform (C) at 65 °C plotted as a function of the (binary) solvent's composition. Lines are predictions using the three models for the binary BC from Tab. 1. The solid, dotted, dashed lines are solutions 1, 2, 3, respectively. For the system AC the second solution from Tab. 1 is used.

This amplification may lead also to dramatic differences in results of process simulations. For demonstration, we have implemented a simulation of a process to separate acetone, benzene, and chloroform as described in [16]. The flowsheet in Fig. 7 is adopted from [16]. Acetone and chloroform, which exhibit a high-boiling azeotrope, are

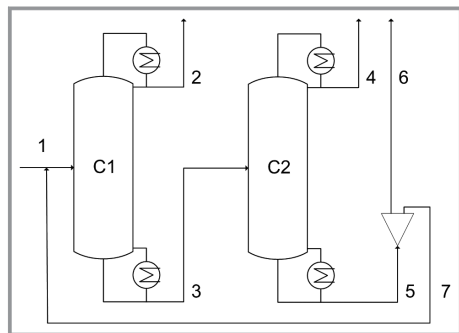


Figure 7. Flowsheet for the separation process for a mixture of acetone, benzene, chloroform.

separated by adding benzene as an entrainer. In column C1, acetone is obtained as top product with high purity. In column C2, chloroform is separated from benzene and obtained in the top product with purity. Benzene obtained at the bottom of column C2 is partly purged and partly recycled. The simulation is done with the software Aspen Plus and the equilibrium stage model for distillation columns (RadFrac). The VLE is modeled as described above. The specifications are given in Tab. 2. There is one degree of freedom left in the simulation resulting from the splitter: the flow rate of the recycle stream 5. In our study, the recycle stream is chosen such that the sum of both reboiler duties is minimized. The calculations are done separately for all six combinations of the three solutions in system BC and the first two solutions in the system AC from Tab. 1. (The last solution of AC is omitted since it is quite distinct when only looking at binary activity coefficients, cf. Fig. 3.)

Table 2. Specifications used in the simulation of the separation process for a mixture of acetone, benzene, chloroform shown in Fig. 7 [16].

Quantity	Value
Pressures (everywhere) [bar]	1.01325
Feed molar flow rate (A, B, C) [kmol h ⁻¹]	36, 40, 24
Feed state	Bubble point 1.01325 bar (66°C)
Number of stages (C1, C2)	68, 60
Feed stage from above (C1, C2)	26, 30
Molar flow rate stream 2 [kmol h ⁻¹]	36
Mole fraction A stream 2 [mol mol ⁻¹]	0.99
Molar flow rate stream 4 [kmol h ⁻¹]	24
Mole fraction C stream 4 [mol mol ⁻¹]	0.98

Experimental VLE data at process pressure (roughly 1 bar) is certainly crucial for the validity of the model. For the system BC one could therefore naively argue that using the data shown in Fig. 4 is sufficient to obtain a good model.

No matter which of the three multiple solution is obtained, the model's performance in binary VLE calculations is seemingly equal. Analogous argumentation holds for the system AC. The results shown in Fig. 8 give, however, a completely different and striking picture: between the different parameter sets used in the simulation, the flow rate of the recycle and the sum of reboiler duties vary between 31 and 155 kmol h⁻¹, and 3.5 and 6.9 MW, respectively. The relative position of the points shows some trend, indicating that both results are connected. The large fluctuations can be explained by the fact that in the bottom of column 1, where traces of acetone have to be separated from a binary mixture of chloroform and benzene, the fluctuations in the activity coefficients discussed along Fig. 6 become significant.

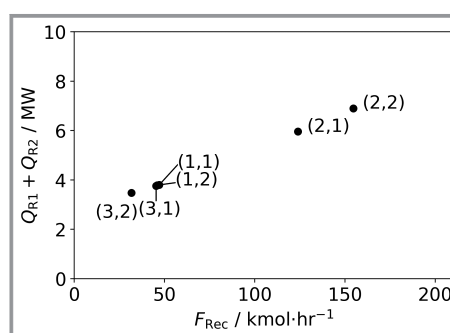


Figure 8. Minimum sum of reboiler duties and respective recycle flow rates for six different parameter combinations. The annotation (i,j) indicates the i -th and j -th solution in the binaries BC and AC, respectively, as given in Tab. 1.

4 Conclusions

Due to the strong nonlinearity of common excess Gibbs energy models like the NRTL model, fitting of binary parameters to vapor-liquid equilibrium data may lead to multiple solutions. They appear as distinct local optima in the optimization of the parameter fitting and may be overlooked if just the global (or one of the local) optimum is calculated. Multiple solutions occur only for binary systems in which the infinite dilution activity coefficients are smaller than 1. In these systems, multiple solutions can be avoided/discriminated when data at different temperatures and/or excess enthalpy data is used in the fit. This has been demonstrated using an exemplary ternary system, which contains two binaries with multiple solutions that are hard to discriminate when only looking at binary VLE data. Multiple solutions, if not eliminated, may yield significant different results when the model is used in predictions of ternary and higher mixtures. Therefore, great attention has to be paid when process simulations are done with systems that exhibit activity coefficients smaller than 1. Even if binary data is modeled well by all the multiple solutions, large differences in results of process simulations are possible.

Open access funding enabled and organized by Projekt DEAL.

Symbols used

F_{Rec}	[kmol h ⁻¹]	recycle flow rate
g^E	[J mol ⁻¹]	molar excess Gibbs energy
Δg	[J mol ⁻¹]	NRTL parameter
h^E	[J mol ⁻¹]	molar excess enthalpy
p	[kPa]	pressure
Q	[MW]	reboiler duty
R	[J mol ⁻¹ K ⁻¹]	universal gas constant
T	[K]	temperature
x	[mol mol ⁻¹]	mole fraction

Greek letters

α	[-]	NRTL parameter
γ	[-]	activity coefficient
γ^∞	[-]	activity coefficient at infinite dilution
τ	[-]	g^E model parameter

Sub- and Superscripts

<i>calc</i>	calculated
<i>exp</i>	experimental

Abbreviations

A	acetone
B	benzene
C	chloroform
MAX	maximum
MIN	minimum
MRV	mid-range value
RDM	relative deviation from the mid-range value
VLE	vapor-liquid equilibrium

References

- [1] H. Renon, J. M. Prausnitz, *AIChE J.* **1968**, *14* (1), 135–144. DOI: <https://doi.org/10.1002/aic.690140124>
- [2] D. S. Abrams, J. M. Prausnitz, *AIChE J.* **1975**, *21* (1), 116–128. DOI: <https://doi.org/10.1002/aic.690210115>
- [3] G. M. Wilson, *J. Am. Chem. Soc.* **1964**, *86*, 127–130. DOI: <https://doi.org/10.1021/ja01056a002>
- [4] S. M. Walas, *Phase Equilibria in Chemical Engineering*, Butterworth-Heinemann, London **1985**.
- [5] C. A. Eckert, S. R. Sherman, *Fluid Phase Equilib.* **1996**, *116*, 333–342. DOI: [https://doi.org/10.1016/0378-3812\(95\)02904-4](https://doi.org/10.1016/0378-3812(95)02904-4)
- [6] E. C. Carlson, *Chem. Eng. Prog.* **1996**, *October*, 35–46.
- [7] S. Sandler, *Fluid Phase Equilib.* **1996**, *116*, 343–353. DOI: [https://doi.org/10.1016/0378-3812\(95\)02905-2](https://doi.org/10.1016/0378-3812(95)02905-2)
- [8] H. Renon, J. M. Prausnitz, *Ind. Eng. Chem. Process Des. Dev.* **1969**, *8* (3), 413–419. DOI: <https://doi.org/10.1021/i260031a019>
- [9] D. Tassios, *Ind. Eng. Chem. Process Des. Dev.* **1979**, *18* (1), 182–186. DOI: <https://doi.org/10.1021/i260069a026>
- [10] N. Silverman, D. Tassios, *Ind. Eng. Chem. Process Des. Dev.* **1977**, *16* (1), 13–20. DOI: <https://doi.org/10.1021/i260061a003>
- [11] K. Miyahara, H. Sadomoto, K. Kitamura, *J. Chem. Eng. Jpn.* **1970**, *3* (2), 157–160. DOI: <https://doi.org/10.1252/jcej.3.157>
- [12] D. A. Palmer, *CRC Handbook of Applied Thermodynamics*, CRC Press, Boca Raton, FL **2019**.
- [13] M. J. Assael et al., *Thermophysical Properties of Fluids: An Introduction to Their Prediction*, Imperial College Press, London **1996**.
- [14] R. C. Reid, J. M. Prausnitz, B. E. Poling, *The Properties of Gases and Liquids*, 4th Ed. McGraw-Hill, New York **1987**.
- [15] M. Bortz et al., *Comput. Chem. Eng.* **2014**, *60*, 354–363. DOI: <https://doi.org/10.1016/j.compchemeng.2013.09.015>
- [16] P. M. Mathias, *Fluid Phase Equilib.* **2016**, *408*, 265–272. DOI: <https://doi.org/10.1016/j.fluid.2015.09.004>
- [17] M. Bortz, J. Burger, N. Aspiron, S. Blagov, K.-H. Küfer, H. Hasse, *Chem. Eng. Sci.* **2015**, *127*, 253–259. DOI: <https://doi.org/10.1016/j.ces.2015.01.044>
- [18] K. Kojima et al., *J. Chem. Eng. Data* **1991**, *36*, 343–345. DOI: <https://doi.org/10.1021/je00003a024>
- [19] E. Forte et al., *AIChE J.* **2018**, *64* (1), 226–237. DOI: <https://doi.org/10.1002/aic.15857>
- [20] E. Forte et al., *Fluid Phase Equilib.* **2020**, *522*, 112676. DOI: <https://doi.org/10.1016/j.fluid.2020.112676>
- [21] I. Nagata et al., *Thermochim. Acta* **1981**, *47* (3), 315–331. DOI: [https://doi.org/10.1016/0040-6031\(81\)80110-4](https://doi.org/10.1016/0040-6031(81)80110-4)
- [22] R. P. Rastogi et al., *J. Chem. Thermodyn.* **1971**, *3* (3), 307–317. DOI: [https://doi.org/10.1016/S0021-9614\(71\)80047-2](https://doi.org/10.1016/S0021-9614(71)80047-2)